TPUPoint: Automatic Characterization of Hardware-Accelerated Machine-Learning Behavior for Cloud Computing

Abenezer Wudenhe and Hung-Wei Tseng University of California, Riverside {awude001, htseng}@ucr.edu

Abstract— With the share of machine learning (ML) workloads in data centers rapidly increasing, cloud providers are beginning to incorporate accelerators such as tensor processing units (TPUs) to improve the energy-efficiency of applications. However, without optimizing application parameters, users may underutilize accelerators and end up wasting energy and money.

This paper presents TPUPoint to facilitate the development of efficient applications on TPU-based cloud platforms. TPUPoint automatically classifies repetitive patterns into phases and identifies the most timing-critical operations in each phase. Further, TPUPoint can associate phases with checkpoints to allow fast-forwarding in applications, thereby significantly reducing the time and money spent optimizing applications.

By running TPUPoint on a wide array of representative ML workloads, we found that computation is no longer the most time-consuming operation; instead, the infeed and reshape operations, which exchange and realign data, become most significant. TPUPoints advantages significantly increase the potential for discovering optimal parameters to quickly balance the complex workload pipeline of feeding data into a system, reformatting the data, and computing results.

I. Introduction

The rise of machine learning (ML) has created a strong demand for efficient ML systems designed for modern cloud-infrastructure applications [1], [2], [3], [4], [5], [6], [7], [8], [9], [10]. Because conventional, general-purpose processors and graphical processing units (GPUs) are optimized for scalar or vector operations, the modern computer architectures that rely on them waste energy when performing ML tasks. More efficient ML accelerators that rely on matrix-based neural networks (NNs) are thus gaining ground in data centers. Googles Tensor Processing Unit (TPU), which offers 70× better performance per watt than conventional GPUs, is by far the most representative case [11].

This paper presents TPUPoint, an open-source toolchair to characterize the behavior and optimize the performance of applications on Google Cloud TPUs. TPUPoints profiler automatically classifies the recurrent patterns of TPU applications into phases and identifies the most timing-critical operations in each phase to inform optimization. TPUPoint can also associate each phase with checkpoints to restart an application

t phase, and TPUPoint gives the user access like the TPUPoint-Optimizer to examine ses with different configurations.

Point at https://github.com/escalab/TPUPoint

pdfelement 試用版

In this paper, we show how TPUPoint may be used to characterize a set of popular ML workloads. We demonstrate that the iterative nature of NN models means that all ML workloads exhibit repetitive behavior that can easily be characterized via very few important phases. TPUPoint identifies time-consuming operators, such as infeed, outfeed, and reshape, that are commonly used among almost all NN models and are not directly related to computation; such indirect operators block the progress of computation if they cannot prepare datasets or swap out datasets fast enough.

As performance characteristics differ among heterogeneous architectural components and platforms, creating uniformly optimized ML programs is unrealistic. A more tenable approach is to automate the optimization process itself. The TPUPoint framework does this through the TPUPoint-Optimizer; the TPUPoint-Optimizer automatically and dynamically rewrites code on Cloud TPU platforms to reduce programmer effort. Our results show that optimal parameters dynamically determined using TPUPoint-Optimizer allow a reasonably written TensorFlow program to achieve at least the same level of performance as that achieved through exhaustive programmer optimizations.

By introducing TPUPoint, this paper makes four key contributions; (1) It presents TPUPoint to accelerate the development and optimization of ML applications for emerging ML accelerator-based cloud architectures, (2) It validates TPUPoint functionality with a wide range of ML applications, (3) It identifies the common bottlenecks of ML applications, (4) It details a systematic approach for discovering optimal parameters for ML applications.

The rest of this paper is organized as follows: Section III describes the architecture of TPUs and TPU-based cloud servers. Section IIII introduces TPUPoints design. Sections IV describes TPUPoint-Analyzer's implementation. Section V describes our experimental platform. Section VII reviews insights gained from TPUPoint-Analyzer. Section VIII presents TPUPoint-Optimizer's results. Section VIII provides a summary of related work for context, and Section IX offers concluding comments.

II. TPUs

Google has widely deployed TPUs in its data centers and made TPUs accessible for user applications through Google

Cloud Services. This section briefly describes the capabilities and interfaces of Cloud TPUs.

A. Cloud TPUs

Google offers three different Cloud TPUs. Google uses the first-generation TPU internally for search and inference but makes the second and third-generation TPUs (TPUv2 and TPUv3, respectively) available via the Google Cloud Platform and TensorFlow Research Cloud (TFRC) program [12]. The TPUv2 chip contains two Matrix Units (MXUs), where each MXU is associated with 8 GiB of High Bandwidth Memory (HBM) to deliver a combined theoretical 45 TFLOPS of computation throughput for 200–250 W TDP. Google typically combines four TPUv2s on a single board [13]. TPUv3 contains twice as many MXUs as TPUv2 and twice the HBM.

Google does not disclose many details about the TPUv3 architecture. Nonetheless, the performance-number specifications, which include a capacity of 90 TFLOPS and 32 GB HBM for each chip, suggest that TPUv3 simply leverages more advanced process technologies to place four MXUs within the same chip while maintaining the same level of power consumption as TPUv2.

B. The Cloud TPU Hardware/Software Interface

A Google Cloud TPU is only accessible through a compute instance (Compute Engine) associated with a TPU instance. Along with the Compute Engine VM, a Google Cloud TPU requires cloud storage (Storage Buckets) for training data and model information during execution; the Compute Engine acts as a host, the TPU acts as a coprocessor, and the Storage Buckets act as persistent memory. These components comprise the Cloud TPU architecture.

TensorFlow [14] is another important part of the Cloud TPU equation. Google developed the TensorFlow framework to model and execute ML algorithms on single machines and heterogeneous/distributed systems. Google Cloud TPUs are readily integrated with TensorFlow. TensorFlow makes heavy use of Googles Protocol Buffers (Protobuf) and Googles Remote Procedural Call (gRPC). Both Protobuf and gRPC are crucial to the TensorFlow framework to allow communication to occur across TensorFlow. TensorFlow makes heavy use of Googles Protocol Buffers (Protobuf) and Googles Remote Procedural Call (gRPC). Protobuf allows for convenient data abstraction across multiple programing languages, and gRPC allows TensorFlow to share data between multiple servers and clients to facilitate execution across multiple devices. The gRPC server implements a method and waits for client requests. A gRPC client uses an object referred to as a stub to provide a channel between the client and server. The stub handles gRPC client requests (with Protobuf) and server responses and uses efficient formats such as RDMA

between processes during execution. Both C are crucial to the TensorFlow framework. cution involves a client (the user), a master, orker processes. The client interacts with the ster coordinates the workers. The master is

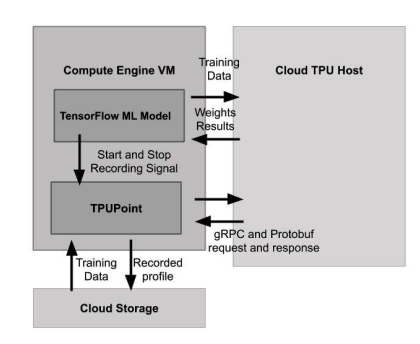


Fig. 1. The TPUPoint system architecture

responsible for handling device placement of graph nodes and partitions the graph into subgraphs to be executed by the workers. In addition to managing the entire computational graph, the master applies optimizations such as constant folding. The workers handle requests from the master, execute kernel operations, and manage communication between kernels.

Even though the Cloud TPUs implementation is not fully available to the public, registered API calls and serviceable requests are still available; a command-line tool called CLOUD-TPU-PROFILER may be used to generate a client-to-master gRPC call that requests a Cloud TPU profile for a small iteration. CLOUD-TPU-PROFILER is limited in its usefulness, however, because it cannot be integrated into training code, only permits insights to be gained post-execution, and only runs within a limited time range (and so cannot profile program execution in its entirety).

III. TPUPOINT-PROFILER: THE CORE OF TPUPOINT

TPUPoint offers a set of tools via the TPUPoint-Profiler module. TPUPoint-Profiler measures Cloud TPU performance and enables the other two elements of the TPUPoint toolchain: (1) TPUPoint-Analyzer (Section [V]), a post-execution, offline analysis tool that identifies the most important application phase and the cause of under-utilized system components and (2) TPUPoint-Optimizer (Section [VII]), the online, automatic workload-optimization tool that dynamically adjusts and rewrites code running on Cloud TPU platforms. This section introduces the TPUPoint design and programming interface.

A. TPUPoint-Profiler Design

The complete TPUPoint toolchain consists of a set of extensions to the TensorFlow framework (the only programming interface for Cloud TPUs at this point). Figure 1 shows the interactions of the core TPUPoint-Profiler that drives TPUPoint-Analyzer and TPUPoint-Optimizer to work with a TensorFlow application.

TPUPoint creates a separate profiling thread upon initialization of the TPUPoint-Profiler. Once created, the TPUPoint-Profiler thread periodically sends profile requests to associated Cloud TPUs independently of the main TensorFlow thread, allowing TPU training to continue uninterrupted while profiling takes place. When a Cloud TPU sends a response back to the profiling thread, TPUPoint-Profiler generates a profile record



```
import tensorflow as tf
2
   from tensorflow.contrib.tpu import TPUPoint as TP
4
   def main(argy):
        estimator = tf.contrib.tpu.TPUEstimator(...)
        tpprofiler = TP(...)
        tpprofiler.Start(analyzer = true)
10
        estimator.train(...)
11
        tpprofiler.Stop()
12
        if __name__ == "__main__":
13
            tf.app.run()
```

Fig. 2. Example TensorFlow code that initiates TPUPoints profiling feature

containing operations along with meta-data of TPU idle time and MXU utilization provided with each response.

If the programmer intends to use TPUPoint-Analyzer, the TPUPoint-Profiler thread will create an additional recording thread to store the collected statistical information in Cloud Storage (otherwise, TPUPoint-Profiler simply buffers the profile in the host main memory). While the recording thread is storing data, TPUPoint-Profilers profiling thread continues to request the next profile from the Cloud TPU. Reliably recording all events during a profile period can produce numerous records, as each profile can potentially include a maximum of 1,000,000 events lasting for a maximum duration of 60,000 ms in total elapsed time. By storing only statistical information in a profile, TPUPoint-Profiler reduces memory consumption and accelerates the post-processing in TPUPoint-Analyzer and TPUPoint-Optimizer. Once the TensorFlow application has completed or reached a user-specified breakpoint, TPUPoint-Profilers profiling thread will send out the last request. All TPUPoint-Profiler threads terminate after TPUPoint-Profiler has received and appropriately saved the last profile record response to the Cloud TPUs. The number of profile records generated depend on the duration of the TensorFlow application.

B. The TPUPoint Programming Interface

The current version of TPUPoint presents a Python/TensorFlow-based front end to the programmer with backend features implemented in C++. Figure 2 shows example code that enables TPUPoint-Profiler in a TensorFlow application. The programmer needs to initiate TPUPoint usage by creating a TPUPoint-Profiler object (tpprofiler in line 7 of the example) with appropriate options.

TPU training is executed though TensorFlow's high level TPUEstimator API (lines 6 and 10). If a programmer wishes to use TPUPoint-Analyzer to perform post-analysis, the analyzer flag must be set to true in the Start() function call (line 9); when the analyzer flag is set to false, TPUPoint-Profiler only enables TPUPoint-Optimizer. Once training is complete (i.e., TPUEstimator.train() has

pished). TPLIPoint-Profiler is halted via Stop() function ost-execution analysis has been specified, element example, Stop() will also instantiate the profiling re-

This implementation allows TPUPoint to profile the entire duration of an application, a feature unavailable in the CLOUD-TPU-PROFILER command line tool.

IV. TPUPOINT-ANALYZER: POST-EXECUTION ANALYSIS

To address the challenge of deriving meaningful results from extensive profiling statistics, TPUPoint-Analyzer walks through and summarizes profiles into program *phases*. To address these challenges, TPUPoint implements TPUPoint-Analyzer's post-execution analysis. Each program phase from TPUPoint-Analyzers post-execution processing identifies similar, repetitive program behaviors. Summarizing program behaviors into phases to facilitate analysis, visualization, and checkpointing/restarting for performance optimizations.

A. Profiling Algorithms

To reduce the TPUPoint-Analyzer search space for calculating program-behavior similarities, TPUPoint-Analyzer first leverages the step numbers that Google makes available for Cloud TPUs—step numbers that indicate coarse-grained, repetitive application behaviors. TPUPoint-Analyzer then uses these steps as the basic unit for similarity comparisons and creates visual summarizes for the steps. TPUPoint-Analyzer offers three summarization methods: the conventional *k*-means algorithm [15], [16], Density Based Spatial Clustering of Applications with Noise (DBSCAN) [17], [18], and a lower-overhead online linear-scan (OLS) algorithm. *k*-means and DBSCAN run after all profiling records have been recorded, while OLS is executed during recording (hence the term "online" in it's name).

k-means: We evaluate TPUPoint-Analyzer using the k-means algorithm implementation by using three stages [19]:

- 1) Extract the records from all statistical profiles and aggregate records together using the TPU step numbers. For each step, we define dimensions in terms of TensorFlow operations, the accumulated number of invocations, and total durations. Using principal component analysis (PCA) for dimensional reduction [20], we have at most 100 distinct operations for frequency vector representation.
- 2) Try the k-means clustering algorithm on aggregated steps for values of k ranging from 1 to 15. Each run of k-means produces a clustering that partitions the steps into k different clusters.
- 3) For each cluster $(k = 1, \ldots, 15)$, calculate the sum of squared distances of samples to cluster centers (centroids) for each value of k. Attempt to minimize the sum of squared distances while maximizing the number of clusters (k) using the elbow method.

TPUPoint-Analyzer implements k-means like SimPoint does [19], [21], [22]. SimPoint uses the Bayesian information criterion (BIC) [23] to measure the probability of clustering for a given simulation. Using instructions per cycle (IPC) as the metric, SimPoint compares using clusters rather than full



試用版

simulations for analysis. TPUPoint aims to simulate complete program execution without architectural metrics such as IPC, instead employing the elbow method [24] as a heuristic to cut clustering off when improvement stops increasing significantly (i.e., when the sum of squared distances for a cluster stops improving significantly).

DBSCAN: DBSCAN $\boxed{17}$, $\boxed{18}$ follows the same general approach as k-means but relies on core samples of high-density clusters. DBSCAN provides an alternative method for comparison with k-means. DBSCAN also has three stages:

- Extract the records from all statistical profiles and produce a frequency vector representation as done in kmeans.
- 2) Apply DBSCAN on aggregated steps of 25, requiring a minimum number of samples from 5 to 200. As the minimum increases, the number of produced clusters decreases.
- 3) For each clustering minimum sample size, measure the ratio of the noise by counting the number of unlabeled points to the total number of points. Attempt to minimize noise while maximizing the number of required samples to form a cluster using the elbow method.

OLS: Both k-means and DBSCAN post-process all records after program execution, which requires the system to store large numbers of records and incur high computational overhead due to the dimensional complexity of each record. To address these issues, TPUPoint-Analyzer offers OLS, which identifies similar, consecutive program behaviors that approximate clustering with significantly lower overhead and reduced data-storage needs. With OLS, TPUPoint-Analyzer simply relies on records from the current step, from the previous step, and from two steps ago. OLS has four stages:

- Extract the records from the incoming statistical profiles and group the records together using their step numbers.
 For each step, use all TensorFlow operations in the program as well as the accumulated number of invocations and the total duration of each operation.
- 2) When the program advances to another step, compare the previous step within a profile to its successor step and calculate their similarity using Equation Π Equation Π computes the similarity of two steps as the ratio of the intersection of the set of events from step i-1 and the set of events from step i-2 to the minimum size of the two sets, where step i-1 is the successor of step i-2. (A set of events for a step is defined as all the unique events that occur during that step.)
- 3) If the successor step is similar according to either a user specified threshold or the default threshold (70% group the two steps together into a single wise, associate the later step with a new

pove stages and gradually aggregate consec-



Fig. 3. Visualization of TPUPoint profiling output

utive steps until all steps from the stored profiles have been parsed.

$$StepSimilarity\left(Step_{i-1}, Step_{i-2}\right) = \frac{|Step_{i-1}| \cap |Step_{i-2}|}{\min(|Step_{i-1}|, |Step_{i-2}|)} \quad (1)$$

B. Visualization

TPUPoint-Analyzer produces a JSON file to store the summarized view of application behavior. This file, along with a corresponding CSV file, contains (1) a formatted description of each phase and (2) the TPU and Host CPU operations executed during training steps. The JSON file is compatible with Google Chromes event-profiling tool, chrome://tracing. Figure 3 shows a visualization of TPUPoint-Analyzer output for phases during TPU training from one such file. Each profile recorded is displayed as a small subsection of the overall execution time on the horizontal Profile Breakdown axis. Each phase identified is displayed as a larger subsection of the overall execution time on the horizontal Phase Breakdown axis. Figure 3 displays how each phase can expand over multiple profile records, effectively summarizing the information from each profile. The time markers displayed in Figure 3 are not to scale, as TPUPoint-Analyzer's visualization of the profiles and phases are only a representation, meant to reduce the information a user must consume. Using Chromes controls, a user can zoom in/out of each program phase to see more/less detail from the TPUPoint-Analyzer output.

C. Checkpointing and Restarting

Along with phases, TPUPoint records the closest checkpoint to each phase stored by the TensorFlow model. To identify checkpoints, TensorFlow compares the steps within a phase and finds the checkpoint with the smallest distance from those steps. This approach allows applications to be modified based on a targeted phase and executed without starting from step zero.

V. EXPERIMENTAL METHODOLOGY

To verify the TPUPoint-Profiler and TPUPoint-Analyzer designs and obtain initial insights to assist code optimizations, we ran a set of experiments on the Google Cloud Platform. Each instance consisted of a single host with a 16-core, 2-way SMT Intel Skylake CPU, 104 GB of main memory, and 250 GB of persistent disk [25]. To maintain implementation consistency, all instances used Docker version 19.03.1 and TensorFlow version 1.15 with TPUPoint installed. As mentioned in Section [II] each instance could access both TPUv2 and TPUv3—model implementations running on a single TPU instance such as TPUv2 could run on a single TPUv3 instance without code modifications. However, scaling for multiple TPU implementations "requires significant tuning and

Workload Name	Workload Type	Model	Dataset	Dataset Size	Default Training Parameters
BERT	Natural Language	BERT	Stanford Question Answering Dataset (SQuAD) Microsoft Research Paraphrase Corpus (MRPC) Multi-Genre Natural Language Interface (MNLI) Corpus of Linguistic Acceptability (CoLA)	422.27 MiB 2.85 MiB 430.61 MiB 1.44 MiB	max seq length: 128 train batch size: 32 learning rate: 2e-5 num train epochs: 3
DCGAN	Image Generation	DCGAN	CIFAR 10 MNIST	178.87 MiB 56.21 MiB	batch size: 1024 num shards: 8 train steps: 10000 train steps per eval: 1000 iterations per loop: 100 learning rate: 0.0002
QANet	Q/A Natural Language	QANet	Stanford Question Answering Dataset (SQuAD)	422.27 MiB	train batch size: 32 steps per epoch: 20000 num epochs: 5
RetinaNet	Object Detection	RetinaNet	Common Objects in Context (COCO)	48.49 GiB	train batch size: 64 image size: 640 num epochs: 15 num examples per epoch: 120k
ResNet	Image Classification	ResNet-50	ImageNet	143.38 GiB	Default Network Depth: 50 Train Steps: 112590 Default Batch Size: 1024

TABLE I
WORKLOAD BREAKDOWN AND SPECIFICATIONS

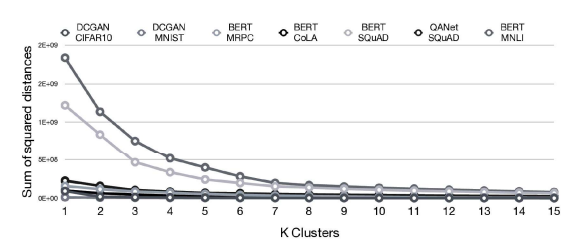


Fig. 4. Clustering results for TPUPoint-Analyzer with scanning based on k-means with different workloads; the plot shows the sum of squared distances of samples to centroids for k clusters (k = 1, ..., 15)

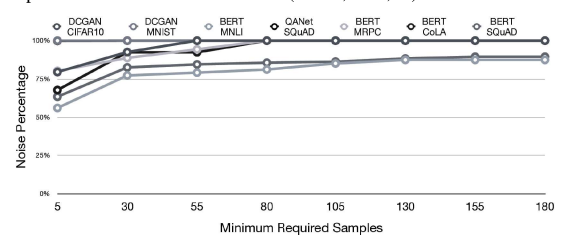


Fig. 5. Clustering results for TPUPoint-Analyzer using DBSCAN with different workloads; the plot shows the ratios of noisy samples to total samples for 5 to 180 minimum required samples to form clusters in steps of 25

optimization" [13]; to avoid any unoptimized model execution, experiments were conducted only on single-TPU instances.

Table I describes the workloads we used to test and verify our designs and hypotheses. We chose publicly available workloads from the TensorFlow 1.14 TPU model library 26: natural language processing (NLP) (BERT 27), image generation (DCGAN 28), question answering (Q/A) NLP (QANet 29), object detection (RetinaNet 30), and image classification(ResNet-50 31).

VI. OBSERVATIONS AND INSIGHTS LEARNED FROM TPUPOINT-ANALYZER

A. Representativeness of Phases

TPUPoint-Analyzer identifies similar, repetitive behaviors in applications and categorizes those behaviors into phases to

by six and optimization. This section discusses and estimate identified from the k-means, DBSCAN, arrang algorithms.

the clustering results for k-means with k inclusive. Each cluster represents a phase

of more extensive program execution. In this case, TPUPoint-Analyzer determines that the sum of squared distances stops improving by a significant margin when k is between 4 and 6; that is, 4 to 6 clusters are sufficient to cover most program behaviors.

Although DBSCAN and k-means both use the elbow method, DBSCAN does not use centroids, so distance cannot be used as a clustering metric. Instead, DBSCAN varies the number of minimum required samples to form a cluster—designating a sample as either a cluster or a noisy sample. Figure $\boxed{5}$ shows the ratio of noisy samples to all samples for the minimum number of required samples ranging from 5 to 180 in aggregated steps of 25. The elbow method was applied in attempt to reduce the noise percentage while maximizing the minimum number of samples required to form a cluster. Using DBSCAN, TPUPoint-Analyzer found that a minimum of 30 to 80 samples was optimal to reduce noise and produced between 3 to 13 clusters. Again, each cluster represents a phase of more extensive program execution.

Figure 6 shows the number of phases that OLS identifies for varying similarities using Equation 1 With a similarity threshold of 70%, we found that most workloads are condensed into just 3 phases. For a similarity threshold above 70%, the number of phases identified grows significantly for the majority of the workloads. For these workloads, we further examined the operators within neighboring phases that cannot combine together, and we found the differences between neighboring phases are essentially ignorable, as they often represent a small amount of the application's execution time, turning even single operations into a phase—this creates a low similarity between phases and so creates an excessive number phases.

As OLS tends to break up steps with small differences into different phases, a high similarity threshold leads to a significant increase in the number of identified phases. That being said, k-means, DBSCAN, and OLS all aggregate the same set of phases into a single phase. Even when TPUPoint-Analyzer uses the extreme 100% StepSimilarity threshold (meaning that TPUPoint-Analyzer requires all steps in a phase to share exactly the same breakdown of operators), TPUPoint-Analyzer still breaks up most workloads into fewer than 15

pdfelement

試用版

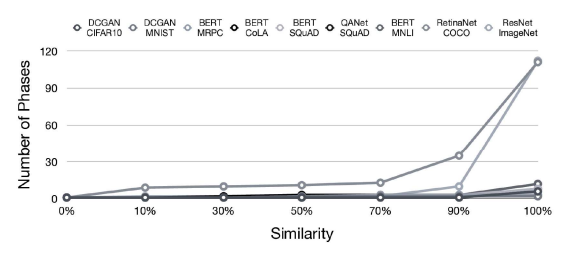


Fig. 6. TPUPoint-Analyzer using OLS with different workloads; the plot shows the number of phases identified with similarity thresholds from 0% to 100%

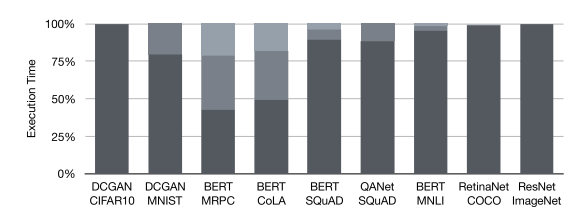


Fig. 7. Coverage of total execution time by the top three phases from TPUPoint-Analyzer using OLS at the 70% similarity threshold with different workloads, where each color represents one of the three identified phases

phases, except for the RetinaNet-COCO and ResNet-ImageNet workloads. The above results give us the first observation for this paper:

Observation 1: most TPU workloads can be summarized into a limited number of phases.

Another metric to judge phase selection is the coverage of execution time. Based on observation 1, we accumulated the total execution time of the 3 longest phases for different threshold values. Figure 7 shows that these top 3 phases encompass at least 95% of the entire execution of each workload at the 70% similarity threshold when using OLS. For the 70% threshold, TPUPoint-Analyzer can cover almost 100% of execution time for all workloads. The results are similar for k-means (k = 5) and DBSCAN (minimum samples = 30), as shown in Figure 9 and Figure 8 respectively. Because of the high number of noisy sample DBSCAN is unable to cluster, we consider these unlabeled samples to be a cluster as well. We find that these represent a majority of most workload's execution time shown in Figure 8. Figure 9 demonstrates that even With k-means set to larger than 3 clusters, will still be dominated by the top 3.

Observation 2: the 3 longest phases cover most of the execution time for TPU workloads.

B. Operators in Phases

Cloud TPUs are simply hardware accelerators in computer systems, so TPU-accelerated workloads still rely on a host program for workload distribution. We now describe the most time-consuming operations on both the host CPU programs and the TPU.

shows the top 5 most time-consuming operations gest phases on both the CPU/host program using TPUv2. For k-means and DB-led phases are mostly identical with nearly top operators. For OLS, which tends to

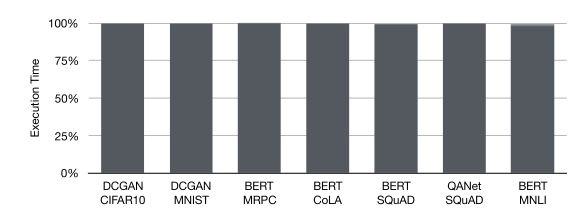


Fig. 8. Coverage of total execution time by the top three phases from TPUPoint-Analyzer using DBSCAN with minimum samples of 30 to form clusters for different workloads, where each color represents one of the three identified phases

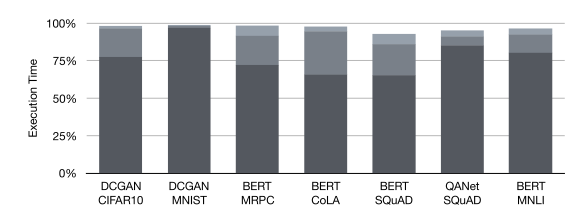


Fig. 9. Coverage of total execution time by the top three phases from TPUPoint-Analyzer using k-means with k=5 for different workloads, where each color represents one of the three identified phases

divide similar phases into multiple phases, the top 5 operators are slightly different from the top 5 k-means and DBSCAN operators.

Differences notwithstanding, all three algorithms identify a common set of the most time-consuming operators on TPUv2 across workloads, with the fusion operator being the most time-consuming overall. The identified fusion operator combines compute-intensive operations from the XLA compiler and is intended to help reduce memory operations [32]. The reshape operator is also one of the most time-consuming operators. Unlike fusion, reshape is not algorithm-related, but rather serves only to prepare input data for subsequent TPU computations.

The most critical operators on the host side TransferBufferToInfeedLocked and OutfeedDequeueTuple. Both operators exchange data with TPUs. Figure 10 shows the percentage of idle time on TPUs for each workload; the Cloud TPUs are, on average, idle for 38.90% of the time for TPUv2 and 43.53% of the time for TPUv3. Figure [11] explores the underutilization of the MXUs—on average, from 22.72% for TPUv2 to 11.34% for TPUv3. During idle time, the host is busy preparing and sending data with the top operators listed in Table II We now have two additional observations:

Observation 3: current TPU workloads incur a significant amount of overhead from data preparation and data exchange. Observation 4: improving TPU data-preparation and TPU data-exchange efficiency on the host computer is key to improving TPU utilization and TPU workload performance.

To identify the differences between Cloud TPUs, we repeated our analysis with the same workloads, datasets, and parameters with TPUv3. Using OLS, *k*-Means, and DBSCAN, we identified the top five operators for the longest identified phase and corresponding cluster. Table III also shows that

			BERT BERT				BE	RT		BERT			DCGAN			DC	GAN		QANet			RetinaNet			esNet				
		MRPC		SQuAD			CoLA			MNLI			CIFAR10			MNIST			SQuAD		COCO		I	ImageNet		Total TPUv2	Total TPUv3		
			k-means	DBSCAN	OLS	k-means	DBSCAN	STO	k-means	DBSCAN	STO	k-means	DBSCAN	OLS	k-means	DBSCAN	OLS	k-means	DBSCAN	STO	k-means	DBSCAN	STO	k-means	OLS	k-means	DBSCAN	Total TPUV2	Total TPOVS
Host Operations	OutfeedDequeueTuple TransferBufferToInfeedLocked RunGraph Send Linearizex32 LSRAv2 InfeedEnqueueTuple InitializeHosForDistributedTpu Restorev2 DisconnectHostFromDistributedTPUSystem Recv Maximum Minimum Sub Cast DecodeAndCropJeg ResizeBicubic StartProgram BuildPaddedOutput	OLS	♦ ♦ ♦ ♦	♦ ♦ ♦ ♦	0			0 0 0 0 0	0 0 0 0	○◇□□	♦ ♦ ♦ ♦ ♦ ♦ ♦ ♦ ♦ ♦ ♦ ♦ ♦ ♦ ♦ ♦ ♦ ♦ ♦			◇◇◇			0		♦ ♦०□□ 0 0	♦ ♦ • • • • • • • • • • • • • • • • • •	♦♦♦	♦	• • • • • • • • • • • • • • • • • • • •			> > > > >		21 19 15 10 9 8 8 7 4 4 4 3 1 1 1 1 1 1 1 0 0	17 17 9 9 15 9 8 3 6 0 1 1 1 0 1 1 1 2 3
TPU Operations	fusion MatMul Reshape L2Loss Conv2DBackpropFilter Mul Transpose Bins.AddGrad Conv2DBackproplinut FusedBatchNormV3 Infeed all-reduce Sum Copy InfeedDequeueTuple FusedBatchNormGradV3 Relu	***	*	*	***	*	*	*	*	*	♦	*	*				◊◊□ 0 ◊0 □	◊◊□ 0 ◊0 □	□ ○◇ ○ □◇◇	* * *	* *		♦ 0 ♦ ♦♦□			> >		23 15 15 12 8 6 6 6 6 5 3 3 3 1 1	23 15 18 12 4 6 6 6 6 3 5 6 3 3 1 1 2

TABLE II

The top 5 most time-consuming operators in the most time-consuming phase using different phase-detection algorithms with TPUv2, shown with \Box , and \Diamond for both.

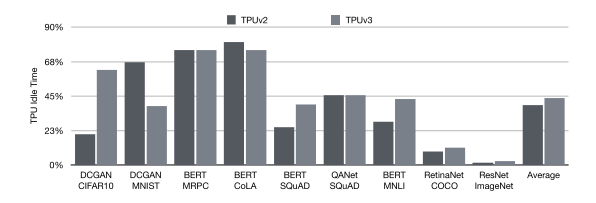


Fig. 10. Idle time for TPUv2 and TPUv3 across workloads

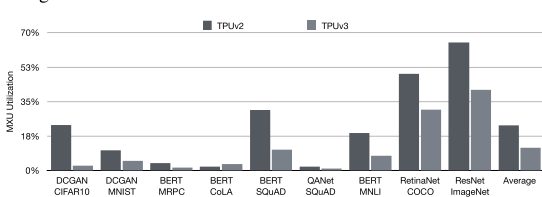


Fig. 11. MXU utilization for TPUv2 and TPUv3 across workloads

the top five operators generally remain consistent for TPUv2 and TPUv3 (as well as the host). Notably, *k*-Means and DBSCAN reach memory limitations for larger workloads such as RetinaNet and ResNet, which affirms that the TPUPoint-Analyzer/OLS combination can compete with clustering methods implemented in SimPoint [21], [22].

For TPUv3, the most time-consuming operators are the same as those for TPUv2 across workloads, but the total utilization of TPU resources changes. The QANet and RetinaNet workloads reduce flop utilization from about 16% on TPUv2 to 13% on TPUv3 for QANet and from about 46%

on TPUv3 for RetinaNet. The increased required for infeed operations indicates ted to memory operators such as outfeed fully utilize TPUv3. However, the observed ainly due to the improved computational

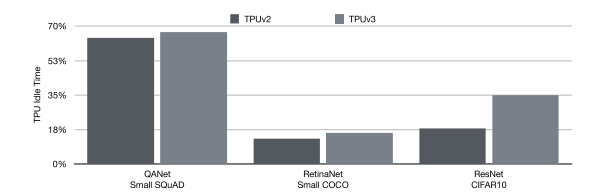


Fig. 12. Idle time for TPUv2 and TPUv3 across QANet, RetinaNet, and ResNet using smaller datasets

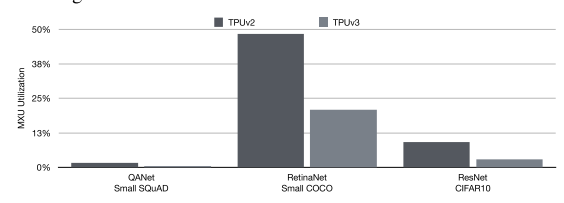


Fig. 13. MXU utilization for TPUv2 and TPUv3 across QANet, RetinaNet, and ResNet using smaller datasets

capabilities of TPUv2 over TPUv3. The increased percentage of time observed for infeed implies that the non-computational overhead in the later-generation TPUs may be more significant.

Observation 5: the significance of non-computational overhead increases as computational throughput improves.

C. Datasets

For the BERT and DCGAN workloads, we used different datasets to help understand the impact of inputs on the associated models. For BERT workloads with 4 different input datasets, the top 5 operators in Table III the TPU idle time in Figure IO and the MXU utilization in Figure III are different, just as they are different for the two workloads that use the DCGAN model.



To further observe model behavior across datasets sizes, QANet, RetinaNet, and ResNet were ran with reduced datasets. QANet and RetinaNet were ran by reducing their original SQuAD and COCO datasets in half. ResNet was ran using the CIFAR10 dataset. Figure 12 and Figure 13 display the idle TPU time and matrix utilization percentage respectively. All models experience a reduction in MXU utilization, and an increase in idle time percentage overall. ResNet in particular experiences the greatest change from it's original ImageNet dataset observations in Figure 10 and Figure 11 even though using the same methodology to feed in the CIFAR10 dataset. These observations provide another insight into performance tuning for ML applications: Observation 6: the performance bottleneck can change as the

Observation 6: the performance bottleneck can change as the input dataset changes, even with the same model.

Observation 6 implies that if a programmer optimizes a program with a specific model using a certain dataset, that optimization may not carry over to different datasets. Observation 6 thus points to the need for dynamic runtime optimization to achieve the best performance for ML workloads.

VII. TPUPOINT-OPTIMIZER

Based on the observations from TPUPoint-Profiler, we designed TPUPoint-Optimizer, an automatic tool that helps to fine-tune the performance of an identified phase in a workload. TPUPoint-Optimizer works without programmer input and ensures that tuning does not affect program-execution output. TPUPoint-Optimizer does the following to help optimize a workload: (1) It analyzes code and automatically instruments code to assist optimization. (2) It allows for online tuning without the need for complete program execution. (3) It controls the output quality. This section describes the design of TPUPoint-Optimizer.

A. Program Analysis

If the user enables TPUPoint-Optimizer, TPUPoint-Optimizer will analyze a TensorFlow program between the calls to start and stop TPUPoint-Profiler. During the program-analysis phase, TPUPoint-Optimizer first identifies *adjustable parameters* originally defined by the user. These adjustable parameters include buffer size, the number of threads dedicated to an operation, and the order of operations that can be rearranged while maintaining correctness. If any of these adjustable parameters cause errors when altered, TPUPoint-Optimizer will not treat them as adjustable. Using the list of input/output variables and adjustable parameters, TPUPoint-Optimizer instruments code to produce checkpoints before each function call within the profiled program.

B. Online Tuning

TPUPoint-Optimizer provides an online performance-tuning feature that adjusts the performance of TPU workloads without ram to finish a complete execution cycle.

Plement UPoint-Optimizers online tuning algorithm om two observations described in the pre-

servation 1—most TPU workloads can be

1.33

1.00 —

1.00 —

0.67 —

0.33 —

0.00 —

QANet SQUAD RetinaNet COCO

Fig. 14. TPUPoint-Optimizer speedups for TPUv2

summarized into a limited number of phases. Observation 2—the 3 longest phases cover most of the execution time for TPU workloads. Taken together, these observations suggest that optimization of a small portion of program execution can have a significant impact on program execution as a whole.

After TPUPoint-Optimizer analyzes input/output variables and instruments code for checkpointing, it will start running the workload using the normal inputs and default parameters. At the same time, TPUPoint-Optimizer tracks the accumulated execution time in different code segments using the statistical model that we developed for TPUPoint-Profiler. If TPUPoint-Profiler observes the most common pattern of operators described in Section VI (e.g., reshape, infeed, fusion, outfeed) within the most time-consuming phases, or the current phase accounts for more than half of the aggregated execution time, TPUPoint-Optimizer will designate the current code segment as having already entered the performance-critical phase and will optimize accordingly, making sure to maintain correctness.

If performance improves and output does not change, TPUPoint-Optimizer continues adjusting parameter values in the same direction until an optimal value for that specific parameter is found. If no other neighboring values are better than the default value, TPUPoint-Optimizer will keep the default value. Finally, TPUPoint-Optimizer uses the improved adjusted parameters to complete rest of the program's execution.

C. Performance of TPUPoint-Optimizer

Figure 14 shows optimized program performance after using TPUPoint-Optimizer to adjust the default parameters and the execution times on TPUv2 (for naive implementations). Figure 14 only shows the workloads that originally took twenty minutes or more to completeother workloads with much shorter execution times (e.g., DCGAN and BERT) show minimal performance gains from TPUPoint-Optimizer and can actually take a performance hit by waiting for TPUPoint-Optimizer to complete any post processing tasks. Using the default parameters from TPUv2, the workloads with long execution times achieve a speedup of about 1.12× on average.

It's important to note that most of the publicly available ML workloads used in this study were manually optimized by Google engineers. So to test TPUPoint-Optimizer, we developed an original naive implementation to see if TPUPoint-Optimizer could improve poor performance. Figure 15 displays TPU idle time of the naive implementation with and



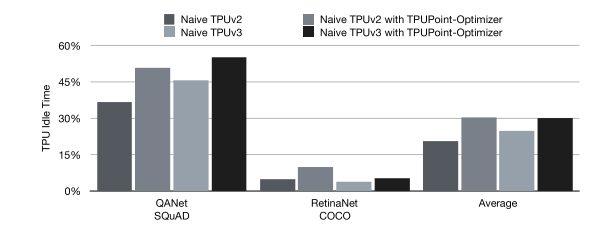


Fig. 15. Idle time for TPUv2 and TPUv3 across workloads optimized with TPUPoint

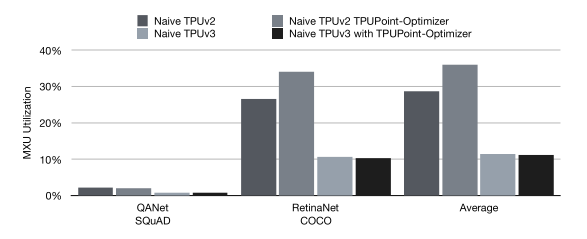


Fig. 16. $\,$ MXU utilization for TPUv2 and TPUv3 across workloads optimized with TPUPoint

without TPUPoint-Optimizer for both TPUv2 and TPUv3. Figure 16 displays the MXU utilization of the naive implementation with and without TPUPoint-Optimizer for both TPUv2 and TPUv3. TPUPoint-Optimizer increased the TPU idle time of the naive implementation for both TPUv2 and TPUv3 (Figure 15) and increased MXU utilization for TPUv2 (Figure 16). Thus, TPUPoint-Optimizer is able to yield performance gains from more efficient use of Cloud TPUs with TPUv2 exhibiting a pronounced change matrix-operation reliance.

When we applied TPUPoint-Optimizer to our naive workloads that originally had execution times of less than twenty minutes (BERT and DCGAN), the workloads showed no notable change in speed compared to their original performance. In contrast, when we applied TPUPoint-Optimizer to our naive workloads that originally took more than twenty minutes (QANet and RetinaNet), we did see improvements in speed—not surprising given that the workloads with longer execution times involve larger and more complex datasets and deeper implementations relative to the workloads with shorter execution times. Because TPUv3 simply contains twice as many MXUs and HBM as TPUv2, we did not observe performance gains from TPUPoint-Optimizer for TPUv3. In fact, we observed an average performance loss under 10% due to the overhead of our profiling/optimization tools. Nonetheless, these results indicate that the overhead associated with TPUPoint-Optimizer is relatively insignificant compared with the overhead associated with complete program execution.

VIII. RELATED WORK

Targeting architectural simulation instead of full-system profiling (the key concept of SimPoint [19], [21], [22]) and program behaviors into program phases (as)) inspired the development of TPUPoint. corporates the checkpointing and restarting MARTS [34] to save time when undertak-

ing architectural simulation and to reduce the cost of cloud computing.

Both TPUPoint and ParaDnn [35] offer tools and systematic methodologies to analyze Cloud TPU performance. TPUPoint provides direct feedback to programmers while automatically and implicitly rewriting under-performing code. In contrast, ParaDnn focuses on systematic testing and optimization insight on architectural perspectives and is therefore complementary to TPUPoint.

In addition to using Cloud TPUs, data centers have often relied on heterogeneous hardware components to accelerate ML workloads [36], [37], [38], [39], [40], [41], [42], [43], [44], [45], [46], [47], [48], [49], [50], [51], [52], [53]. However, hardware solutions are generally not distribution friendly. As TPUPoint works at the programming-language/application level to observe and optimize performance, TPUPoint is portable; simply changing the low-level library function calls that TPUPoint uses to retrieve statistics makes TPUPoints profiling and optimization available on a wide variety of platforms.

Some benchmark suites also attempt to standardize ML workload management: μ Suite [54], BigDataBench [55], AI Benchmark [56], EEMBC MLMark Benchmark [57], [58], Fathom [59], AI Matrix [60], DeepBench [61], DAWN-Bench [62], and MLPerf [63], and mixed-precision benchmarks as well [64], [65]. When benchmarking Cloud TPUs, we can only test a subset of each benchmark suite due to the limited front-end programming-language support for the Cloud TPU platform. That being said, many benchmarks rely on the same models and datasets, varying only frameworks and implementations. We have tried our best to cover the spectrum of ML workloads.

There have been several prior papers on summarizing ML such as EcoRNN [66], SeqPoints [67], and TBD [68]. These works do not attempt to profile/optimize the same range of benchmarks as TPUPoint does, where computation could be input independent or heterogeneous across iterations. EcoRNN and TBD take a sampling and iteration-based approach to LSTM RNN and DNN respectively, while SeqPoint considers how input variation effects sequence-based neural networks (SQNNs). To provide insight to such a wide range of ML workloads, TPUPoint aims for high coverage but low overhead regardless of the ML workload.

As ML workloads predominate in cloud services, methods for optimizing resource utilization have received significant attention. Some methods use performance estimation algorithms [69], [70], [71], [72], [73] or training models [74], [75], [76] to select optimal parameters. Such methods tend to have stagnant selectors, and while they offer lower overhead, they are limited in their ability to adapt to new workloads. Instead of focusing only on a specific workload, TPUPoint provides a more generic framework applicable to a much broader range of ML tasks.

IX. CONCLUSION

This paper presents TPUPoint, a toolchain that collects, an-

alyzes, and optimizes the performance of TPU-accelerated ML workloads. Using the post-analysis tool, TPUPoint-Analyzer, we determined that most TPU-accelerated ML workloads are under-utilizing precious TPU resources. Moreover, because workload behavior varies by model and dataset, manually optimizing workloads is not feasible. Fortunately, the behavior within a workload is often repetitive, opening the door for dynamic optimizations. Using the observations learned from TPUPoint-Analyzer, we designed TPUPoint-Optimizer to detect the main application phase and dynamically adjust parameters in running code. Our results show a $1.12 \times$ speedup over default parameters without programmer intervention.

ACKNOWLEDGMENTS

The authors would like to thank the anonymous reviewers for their helpful comments. We want to thank TensorFlow Research Cloud (TFRC) for providing us access and support for clouds TPUs. We also owe a debt of gratitude to Christopher Fraser for his excellent copyediting skills. This work was sponsored by National Science Foundation (NSF) award, CNS-2007124.

REFERENCES

- Y. Deng, F. Bao, Y. Kong, Z. Ren, and Q. Dai, "Deep direct reinforcement learning for financial signal representation and trading," *IEEE Transactions on Neural* Networks and Learning Systems, vol. 28, no. 3, pp. 653–664, 2017.
- [2] X. Ding, Y. Zhang, T. Liu, and J. Duan, "Deep learning for event-driven stock prediction," in *Proceedings of the 24th International Conference on Artificial Intelligence*, ser. IJCAI'15. AAAI Press, 2015, p. 23272333.
- [3] A. Grover and J. Leskovec, "Node2vec: Scalable feature learning for networks," in Proceedings of the 22nd ACM SIGKDD International Conference on Knowledge Discovery and Data Mining, ser. KDD '16. New York, NY, USA: Association for Computing Machinery, 2016, p. 855864. [Online]. Available: [https://doi.org/10.1145/2939672.2939754]
- [4] T. N. Kipf and M. Welling, "Semi-supervised classification with graph convolutional networks," arXiv, 2017.
- [5] X. Liu, H. Yang, Z. Liu, L. Song, H. Li, and Y. Chen, "DPatch: An adversarial patch attack on object detectors," arXiv, 2019.
- [6] W. Liu, D. Anguelov, D. Erhan, C. Szegedy, S. Reed, C.-Y. Fu, and A. C. Berg, "SSD: Single shot multibox detector," in *Computer Vision – ECCV 2016*, B. Leibe, J. Matas, N. Sebe, and M. Welling, Eds. Cham: Springer International Publishing, 2016, pp. 21–37.
- [7] B. Perozzi, R. Al-Rfou, and S. Skiena, "DeepWalk: Online learning of social representations," in *Proceedings of the 20th ACM SIGKDD International Conference on Knowledge Discovery and Data Mining*, ser. KDD '14. New York, NY, USA: Association for Computing Machinery, 2014, p. 701710. [Online]. Available: https://doi.org/10.1145/2623330.2623732
- [8] S. Ren, K. He, R. Girshick, and J. Sun, "Faster R-CNN: Towards real-time object detection with region proposal networks," in Advances in Neural Information Processing Systems 28, C. Cortes, N. D. Lawrence, D. D. Lee, M. Sugiyama, and R. Garnett, Eds. Curran Associates, Inc., 2015, pp. 91–99. [Online]. Available: http://papers.nips.cc/paper/5638-faster-r-cnn-towards-real-time-object-detection-with-region-proposal-netwo-kspdf
- [9] L. Song, F. Chen, S. R. Young, C. D. Schuman, G. Perdue, and T. E. Potok, "Deep learning for vertex reconstruction of neutrino-nucleus interaction events with combined energy and time data," in ICASSP 2019 - 2019 IEEE International Conference on Acoustics, Speech and Signal Processing (ICASSP), 2019, pp. 3882– 3886.
- [10] R. Miotto, F. Wang, S. Wang, X. Jiang, and J. T. Dudley, "Deep learning for healthcare: review, opportunities and challenges," *Briefings in Bioinformatics*, vol. 19, no. 6, pp. 1236–1246, 05 2017. [Online]. Available: https://doi.org/10.1093/bib/bbx044
- [11] N. P. Jouppi, C. Young, N. Patil, D. Patterson, G. Agrawal, R. Bajwa, S. Bates, S. Bhatia, N. Boden, A. Borchers, R. Boyle, P.-l. Cantin, C. Chao, C. Clark, J. Dean, B. Gelb, T. V. Ghaemmaghami, Bland, R. Haemann, C. R. Ho, D. Hogberg, J. Hu, R. Hundt, J. L. Barmann, C. R. Ho, D. Hogberg, J. Hu, R. Hundt, J. Barmann, C. R. Ho, D. Hught, J. Barmann, C. R. Ho, D. Hogberg, J. Hu, R. Hundt, J. Barmann, C. R. Ho, D. Hogberg, J. Hu, R. Hundt, J. Barmann, C. R. Ho, D. Hught, J. Barmann, C. R. Hundt, J. Barmann, C. R. Hundt, J. Barmann, C. R. Hundt, J. Barmann, C. R. H
 - lland, R. Hagmann, C. R. Ho, D. Hogberg, J. Hu, R. Hundt, Jaffey, A. Jaworski, A. Kaplan, H. Khaitan, D. Killebrew, S. Lacy, J. Laudon, J. Law, D. Le, C. Leary, Z. Liu, K. Lucke, Kean, A. Maggiore, M. Mahony, K. Miller, R. Nagarajan, R. Ni, K. Nix, T. Norrie, M. Omernick, N. Penukonda, M. Ross, A. Salek, E. Samadiani, C. Severn, G. Sizikov,

- M. Snelham, J. Souter, D. Steinberg, A. Swing, M. Tan, G. Thorson, B. Tian, H. Toma, E. Tuttle, V. Vasudevan, R. Walter, W. Wang, E. Wilcox, and D. H. Yoon, "In-datacenter performance analysis of a Tensor Processing Unit," in *Proceedings of the 44th Annual International Symposium on Computer Architecture*, ser. ISCA '17. New York, NY, USA: Association for Computing Machinery, 2017, p. 112. [Online]. Available: [https://doi.org/10.1145/3079856.3080246]
- [12] (2020) Tensorflow research cloud. [Online]. Available: https://www.tensorflow.org/tfrc
- [13] Google Cloud. (2020) System architecture cloud TPU. [Online]. Available: https://cloud.google.com/tpu/docs/system-architecture
- [14] TensorFlow. [Online]. Available: https://github.com/tensorflow/tensorflow
- [15] S. Lloyd, "Pleast squares quantization in PCM," *IEEE Transactions on Information Theory*, vol. 28, no. 2, pp. 129–137, 1982.
- [16] J. Macqueen, "Some methods for classification and analysis of multivariate observations," *Multivariate Observations*, p. 17, 1967.
- [17] M. Ester, H.-P. Kriegel, J. Sander, and X. Xu, "A density-based algorithm for discovering clusters in large spatial databases with noise," in KDD, 1996, pp. 226– 231. [Online]. Available: http://www.aaai.org/Library/KDD/1996/kdd96-037.php
- [18] E. Schubert, J. Sander, M. Ester, H. P. Kriegel, and X. Xu, "DBSCAN revisited, revisited: Why and how you should (still) use DBSCAN," ACM Trans. Database Syst., vol. 42, no. 3, Jul. 2017. [Online]. Available: https://doi.org/10.1145/3068335
- [19] T. Sherwood, E. Perelman, G. Hamerly, and B. Calder, "Automatically characterizing large scale program behavior," in *Proceedings of the 10th International Conference on Architectural Support for Programming Languages and Operating Systems*, ser. ASPLOS X. New York, NY, USA: Association for Computing Machinery, 2002, p. 4557. [Online]. Available: https://doi.org/10.1145/605397.605403
- [20] S. Wold, K. Esbensen, and P. Geladi, "Principal component analysis," Chemometrics and Intelligent Laboratory Systems, vol. 2, no. 1, pp. 37 – 52, 1987, proceedings of the Multivariate Statistical Workshop for Geologists and Geochemists. [Online]. Available: http://www.sciencedirect.com/science/article/pii/0169743987800849
- [21] G. Hamerly, E. Perelman, and B. Calder, "Comparing multinomial and k-means clustering for SimPoint," in 2006 IEEE International Symposium on Performance Analysis of Systems and Software, 2006, pp. 131–142.
- [22] E. Perelman, M. Polito, J. . Bouguet, J. Sampson, B. Calder, and C. Dulong, "Detecting phases in parallel applications on shared memory architectures," in *Proceedings 20th IEEE International Parallel Distributed Processing Symposium*, 2006, p. pp. 10.
- [23] D. Pelleg and A. Moore, "X-means: Extending K-means with efficient estimation of the number of clusters," in *Proceedings of the 17th International Conf. on Machine Learning*, 2000, p. 727734.
- Machine Learning, 2000, p. 727734.

 [24] R. L. Thorndike, "Who belongs in the family?" *Psychometrika*, vol. 18, no. 4, pp. 267–276, Dec 1953. [Online]. Available: https://doi.org/10.1007/BF02289263
- [25] Gogle Cloud. (2020) Machine Types Compute Engine Documentation. [Online]. Available: https://cloud.google.com/compute/docs/machine-types
- [26] TensorFlow. (2019) TensorFlow TPU models. [Online]. Available: https://github.com/tensorflow/tpu
- [27] I. Turc, M.-W. Chang, K. Lee, and K. Toutanova, "Well-read students learn better: On the importance of pre-training compact models," arXiv. 2019.
- On the importance of pre-training compact models," arXiv, 2019.

 [28] A. Radford, L. Metz, and S. Chintala, "Unsupervised representation learning with deep convolutional generative adversarial networks," arXiv, 2016.
- [29] A. W. Yu, D. Dohan, M.-T. Luong, R. Zhao, K. Chen, M. Norouzi, and Q. V. Le, "QANet: Combining local convolution with global self-attention for reading comprehension," arXiv, 2018.
- [30] T.-Y. Lin, P. Goyal, R. Girshick, K. He, and P. Dollar, "Focal loss for dense object detection," in *Proceedings of the IEEE International Conference on Computer Vision (ICCV)*, Oct 2017.
- [31] K. He, X. Zhang, S. Ren, and J. Sun, "Deep residual learning for image recognition," *CoRR*, vol. abs/1512.03385, 2015. [Online]. Available: http://arxiv.org/abs/1512.03385
- [32] TensorFlow. (2020) XLA: Optimizing compiler for machine learning. [Online]. Available: https://www.tensorflow.org/xla
- [33] M. Yan, L. Deng, X. Hu, L. Liang, Y. Feng, X. Ye, Z. Zhang, D. Fan, and Y. Xie, "HyGCN: A GCN accelerator with hybrid architecture," in 2020 IEEE International Symposium on High Performance Computer Architecture (HPCA), 2020, pp. 15–29.
- [34] T. F. Wenisch, R. E. Wunderlich, B. Falsafi, and J. C. Hoe, "TurboSMARTS: Accurate microarchitecture simulation sampling in minutes," in *Proceedings of the 2005 ACM SIGMETRICS International Conference on Measurement and Modeling of Computer Systems*, ser. SIGMETRICS '05. New York, NY, USA: Association for Computing Machinery, 2005, p. 408409. [Online]. Available: https://doi.org/10.1145/1064212.1064278
- [35] Y. Wang, G.-Y. Wei, and D. Brooks, "A systematic methodology for analysis of deep learning hardware and software platforms," in *Proceedings of Machine Learning and Systems*, I. Dhillon, D. Papailiopoulos, and V. Sze, Eds., vol. 2, 2020, pp. 30–43. [Online]. Available: https://proceedings.mlsys.org/paper/2020/file/c20ad4d76fe97759aa27a0c99bff6710-Paper.pdf
- [36] J. Fowers, K. Ovtcharov, M. Papamichael, T. Massengill, M. Liu, D. Lo, S. Alkalay, M. Haselman, L. Adams, M. Ghandi, S. Heil, P. Patel, A. Sapek, G. Weisz, L. Woods, S. Lanka, S. K. Reinhardt, A. M. Caulfield, E. S. Chung, and D. Burger, "A configurable cloud-scale DNN processor for real-time AI," in 2018 ACM/IEEE 45th Annual International Symposium on Computer Architecture (ISCA), 2018, pp.

- [37] E. Chung, J. Fowers, K. Ovtcharov, M. Papamichael, A. Caulfield, T. Massengill, M. Liu, D. Lo, S. Alkalay, M. Haselman, M. Abeydeera, L. Adams, H. Angepat, C. Boehn, D. Chiou, O. Firestein, A. Forin, K. S. Gatlin, M. Ghandi, S. Heil, K. Holohan, A. El Husseini, T. Juhasz, K. Kagi, R. K. Kovvuri, S. Lanka, F. van Megen, D. Mukhortov, P. Patel, B. Perez, A. Rapsang, S. Reinhardt, B. Rouhani, A. Sapek, R. Seera, S. Shekar, B. Sridharan, G. Weisz, L. Woods, P. Yi Xiao, D. Zhang, R. Zhao, and D. Burger, "Serving DNNs in real time at datacenter scale with project Brainwave," *IEEE Micro*, vol. 38, no. 2, pp. 8–20, 2018.
- [38] H. Esmaeilzadeh, A. Sampson, L. Ceze, and D. Burger, "Neural acceleration for general-purpose approximate programs," in 2012 45th Annual IEEE/ACM International Symposium on Microarchitecture, 2012, pp. 449–460.
- [39] K. Hazelwood, S. Bird, D. Brooks, S. Chintala, U. Diril, D. Dzhulgakov, M. Fawzy, B. Jia, Y. Jia, A. Kalro, J. Law, K. Lee, J. Lu, P. Noordhuis, M. Smelyanskiy, L. Xiong, and X. Wang, "Applied machine learning at Facebook: A datacenter infrastructure perspective," in 2018 IEEE International Symposium on High Performance Computer Architecture (HPCA), 2018, pp. 620–629.
- [40] C. Wu, D. Brooks, K. Chen, D. Chen, S. Choudhury, M. Dukhan, K. Hazelwood, E. Isaac, Y. Jia, B. Jia, T. Leyvand, H. Lu, Y. Lu, L. Qiao, B. Reagen, J. Spisak, F. Sun, A. Tulloch, P. Vajda, X. Wang, Y. Wang, B. Wasti, Y. Wu, R. Xian, S. Yoo, and P. Zhang, "Machine learning at Facebook: Understanding inference at the edge," in 2019 IEEE International Symposium on High Performance Computer Architecture (HPCA), 2019, pp. 331–344.
- [41] S. Markidis, S. W. D. Chien, E. Laure, I. B. Peng, and J. S. Vetter, "NVIDIA Tensor Core programmability, performance precision," in 2018 IEEE International Parallel and Distributed Processing Symposium Workshops (IPDPSW), 2018, pp. 522–531
- [42] L. Durant, O. Giroux, M. Harris, and N. Stam. (2017, May) Inside Volta: The worlds most advanced data center GPU. [Online]. Available: https://developer.nvidia.com/blog/inside-volta/
- [43] C. Zhang, G. Sun, Z. Fang, P. Zhou, P. Pan, and J. Cong, "Caffeine: Toward uniformed representation and acceleration for deep convolutional neural networks," *IEEE Transactions on Computer-Aided Design of Integrated Circuits and Systems*, vol. 38, no. 11, pp. 2072–2085, 2019.
- [44] Y.-H. Chen, J. Emer, and V. Sze, "Eyeriss: A spatial architecture for energy-efficient dataflow for convolutional neural networks," in *Proceedings of the 43rd International Symposium on Computer Architecture*, ser. ISCA '16. IEEE Press, 2016, p. 367379. [Online]. Available: https://doi.org/10.1109/ISCA.2016.40]
- [45] S. Venkataramani, A. Ranjan, S. Banerjee, D. Das, S. Avancha, A. Jagannathan, A. Durg, D. Nagaraj, B. Kaul, P. Dubey, and A. Raghunathan, "ScaleDeep: A scalable compute architecture for learning and evaluating deep networks," in *Proceedings of the 44th Annual International Symposium on Computer Architecture*, ser. ISCA '17. New York, NY, USA: Association for Computing Machinery, 2017, p. 1326. [Online]. Available: https://doi.org/10.1145/3079856. 3080244
- [46] Y. S. Shao, J. Clemons, R. Venkatesan, B. Zimmer, M. Fojtik, N. Jiang, B. Keller, A. Klinefelter, N. Pinckney, P. Raina, S. G. Tell, Y. Zhang, W. J. Dally, J. Emer, C. T. Gray, B. Khailany, and S. W. Keckler, "Simba: Scaling deep-learning inference with multi-chip-module-based architecture," in *Proceedings of the 52nd Annual IEEE/ACM International Symposium on Microarchitecture*, ser. MICRO 52. New York, NY, USA: Association for Computing Machinery, 2019, p. 1427. [Online]. Available: https://doi.org/10.1145/3352460.3358302
- [47] Q. Yu, C. Wang, X. Ma, X. Li, and X. Zhou, "A deep learning prediction process accelerator based FPGA," in 2015 15th IEEE/ACM International Symposium on Cluster, Cloud and Grid Computing, 2015, pp. 1159–1162.
- [48] N. Srivastava, H. Jin, S. Smith, H. Rong, D. Albonesi, and Z. Zhang, "Tensaurus: A versatile accelerator for mixed sparse-dense tensor computations," in 2020 IEEE International Symposium on High Performance Computer Architecture (HPCA), 2020, pp. 689–702.
- [49] A. M. Caulfield, E. S. Chung, A. Putnam, H. Angepat, J. Fowers, M. Haselman, S. Heil, M. Humphrey, P. Kaur, J. Kim, D. Lo, T. Massengill, K. Ovtcharov, M. Papamichael, L. Woods, S. Lanka, D. Chiou, and D. Burger, "A cloud-scale acceleration architecture," in 2016 49th Annual IEEE/ACM International Symposium on Microarchitecture (MICRO), 2016, pp. 1–13.
- [50] T. Moreau, M. Wyse, J. Nelson, A. Sampson, H. Esmaeilzadeh, L. Ceze, and M. Oskin, "SNNAP: Approximate computing on programmable SoCs via neural acceleration," in 2015 IEEE 21st International Symposium on High Performance Computer Architecture (HPCA), 2015, pp. 603–614.
- [51] B. Reagen, P. Whatmough, R. Adolf, S. Rama, H. Lee, S. K. Lee, J. M. Hernndez-Lobato, G. Wei, and D. Brooks, "Minerva: Enabling low-power, highly-accurate deep neural network accelerators," in 2016 ACM/IEEE 43rd Annual International Symposium on Computer Architecture (ISCA), 2016, pp. 267–278.
- [52] T. Chen, Z. Du, N. Sun, J. Wang, C. Wu, Y. Chen, and O. Temam, "DianNao: A small-footprint high-throughput accelerator for ubiquitous machine-learning," in Proceedings of the 19th International Conference on Architectural Support for Programming Languages and Operating Systems, ser. ASPLOS '14. New York, NY, USA: Association for Computing Machinery, 2014, p. 269284. [Online]. iorg/10.1145/2541940.2541967

Liu, S. Zhang, L. He, J. Wang, L. Li, T. Chen, Z. Xu, N. Sun, DianNao: A machine-learning supercomputer," in 2014 47th International Symposium on Microarchitecture, 2014, pp. 609—

F. Wenisch, " μ Suite: A Benchmark Suite for Microservices,"

- in 2018 IEEE International Symposium on Workload Characterization (IISWC), 2018, pp. 1–12.
- [55] L. Wang, J. Zhan, C. Luo, Y. Zhu, Q. Yang, Y. He, W. Gao, Z. Jia, Y. Shi, S. Zhang, C. Zheng, G. Lu, K. Zhan, X. Li, and B. Qiu, "BigDataBench: A big data benchmark suite from internet services," in 2014 IEEE 20th International Symposium on High Performance Computer Architecture (HPCA), 2014, pp. 488–499.
- [56] A. Ignatov, R. Timofte, A. Kulik, S. Yang, K. Wang, F. Baum, M. Wu, L. Xu, and L. Van Gool, "AI Benchmark: All about deep learning on smartphones in 2019," in 2019 IEEE/CVF International Conference on Computer Vision Workshop (ICCVW), 2019, pp. 3617–3635.
- [57] (2019) Introducing the EEMBC MLMark Benchmark. [Online]. Available: https://www.eembc.org/mlmark/
- [58] P. Torelli and M. Bangale, "Measuring inference performance of machine-learning frameworks on edge-class devices with the MLMark Benchmark," White Paper, EEMBC. [Online]. Available: https://www.eembc.org/techlit/articles/MLMARK-WHITEPAPER-FINAL-I.pdf]
- [59] R. Adolf, S. Rama, B. Reagen, G. Wei, and D. Brooks, "Fathom: reference workloads for modern deep learning methods," in 2016 IEEE International Symposium on Workload Characterization (IISWC), 2016, pp. 1–10.
- [60] Alibaba. (2018) AI Matrix. [Online]. Available: https://aimatrix.ai/en-us/
- [61] Baidu. (2017) DeepBench: Benchmarking deep learning operations on different hardware. [Online]. Available: https://github.com/baidu-research/DeepBench
- [62] C. Coleman, D. Narayanan, D. Kang, T. Zhao, J. Zhang, L. Nardi, P. Bailis, K. Olukotun, C. R, and M. Zaharia, "DAWNBench: An end-to-end deep learning benchmark and competition," NIPS ML Systems Workshop, 2017.
- [63] P. Mattson, C. Cheng, G. Diamos, C. Coleman, P. Micikevicius, D. Patterson, H. Tang, G.-Y. Wei, P. Bailis, V. Bittorf, D. Brooks, D. Chen, D. Dutta, U. Gupta, K. Hazelwood, A. Hock, X. Huang, D. Kang, D. Kanter, N. Kumar, J. Liao, D. Narayanan, T. Oguntebi, G. Pekhimenko, L. Pentecost, V. Janapa Reddi, T. Robie, T. St John, C.-J. Wu, L. Xu, C. Young, and M. Zaharia, "MLPerf training benchmark," in *Proceedings of Machine Learning and Systems*, I. Dhillon, D. Papaliliopoulos, and V. Sze, Eds., vol. 2, 2020, pp. 336–349. [Online]. Available: https://proceedings.mlsys.org/paper/2020/file/02522a2b2726fb0a03bb19f2d8d9524d-Paper.pdf
- [64] P. Luszczek, J. Kurzak, I. Yamazaki, and J. Dongarra, "Towards numerical benchmark for half-precision floating point arithmetic," in 2017 IEEE High Performance Extreme Computing Conference (HPEC), 2017, pp. 1–5.
- [65] A. Yazdanbakhsh, D. Mahajan, H. Esmaeilzadeh, and P. Lotfi-Kamran, "AxBench: A multiplatform benchmark suite for approximate computing," *IEEE Design Test*, vol. 34, no. 2, pp. 60–68, 2017.
- [66] B. Zheng, A. Tiwari, N. Vijaykumar, and G. Pekhimenko, "Echo: Compiler-based GPU Memory Footprint Reduction for LSTM RNN Training," 2019.
- [67] S. Pati, S. Aga, M. D. Sinclair, and N. Jayasena, "SeqPoint: Identifying Representative Iterations of Sequence-Based Neural Networks," in 2020 IEEE International Symposium on Performance Analysis of Systems and Software (ISPASS), 2020, pp. 69–80.
- [68] H. Zhu, M. Akrout, B. Zheng, A. Pelegris, A. Jayarajan, A. Phanishayee, B. Schroeder, and G. Pekhimenko, "Benchmarking and Analyzing Deep Neural Network Training," in 2018 IEEE International Symposium on Workload Characterization (IISWC), 2018, pp. 88–100.
- [69] J. Zhang, J. Sun, W. Zhou, and G. Sun, "An active learning method for empirical modeling in performance tuning," in 2020 IEEE International Parallel and Distributed Processing Symposium (IPDPS), 2020, pp. 244–253.
- [70] N. Hasabnis, "Auto-tuning TensorFlow threading model for CPU backend," in 2018 IEEE/ACM Machine Learning in HPC Environments (MLHPC), 2018, pp. 14–25.
- [71] S. J. Kaufman, P. M. Phothilimthana, Y. Zhou, and M. Burrows, "A learned performance model for the Tensor Processing Unit," 2020.
 [72] J. W. Choi, A. Singh, and R. W. Vuduc, "Model-driven autotuning of sparse
- [72] J. W. Choi, A. Singh, and R. W. Vuduc, "Model-driven autotuning of sparse matrix-vector multiply on GPUs," in *Proceedings of the 15th ACM SIGPLAN Symposium on Principles and Practice of Parallel Programming*, ser. PPoPP '10. New York, NY, USA: Association for Computing Machinery, 2010, p. 115126. [Online]. Available: https://doi.org/10.1145/1693453.1693471
- [73] L. Song, F. Chen, Y. Zhuo, X. Qian, H. Li, and Y. Chen, "AccPar: Tensor partitioning for heterogeneous deep learning accelerators," in 2020 IEEE International Symposium on High Performance Computer Architecture (HPCA), 2020, pp. 342–355.
- [74] G. Wang, J. Xu, and B. He, "A novel method for tuning configuration parameters of spark based on machine learning," in 2016 IEEE 18th International Conference on High Performance Computing and Communications; IEEE 14th International Conference on Smart City; IEEE 2nd International Conference on Data Science and Systems (HPCC/Smart/City/DSS), 2016, pp. 586–593.
- [75] S. Bhowmick, V. Eijkhout, Y. Freund, E. Fuentes, and D. Keyes, Application of Alternating Decision Trees in Selecting Sparse Linear Solvers. New York, NY: Springer New York, 2010, pp. 153–173. [Online]. Available: https://doi.org/10.1007/978-1-4419-6935-4_10
- [76] J. Demmel, J. Dongarra, V. Eijkhout, E. Fuentes, A. Petitet, R. Vuduc, R. C. Whaley, and K. Yelick, "Self-adapting linear algebra algorithms and software," Proceedings of the IEEE, vol. 93, no. 2, pp. 293–312, 2005.

pdfelement

試用版